Application of 3D–Seismic Data in Detecting Buried Karsts in Asmari Formation: An Example from Kupal Oil Field, Southwest Iran

Mousa Zohrabzadeh[1], Hossain Rahimpour–Bonab[2]*, Mohsen Aleali[1]
[1] *Department of Geology, Science and Research Branch, Islamic Azad University (IAU), Tehran, Iran*
[2] *School of Geology, College of Science, University of Tehran, Tehran, Iran*
**Corresponding author, e–mail: rahimpor@ut.ac.ir*
(*received: 15/09/2018 ; accepted: 17/12/2018*)

Abstract
Detecting karstification processes in hydrocarbon carbonate reservoirs is extremely important because of their porosity and permeability and also the risk associated with their drilling. A very useful technique to locate buried karsts is 3D seismic. In this research, seismic frequency decomposition (spectral decomposition) and seismic inversion techniques used to identify these sub–surface diagenetic features that control the quality of the Asmari reservoir of the Kupal oil field. The results point to numerous buried karstified features in the upper Asmari which can be regarded as the main targets for reservoir development. According to seismic inversion karstic interval (mainly as channel) have lower seismic acoustic impedance, and at the same time higher effective porosity. Also, numerous geological evidences such as drilling fluid loss, tidal and supratidal facies, as well as the development of fenestrate porosity, vuggy and extended vuggy porosity in the upper Asmari, all point to the meteoric diagenesis and subaerial exposure. These confirm the likelihood of formation of paleokarsts in this part of the Asmari Formation. Therefore, the results of this research can be very useful in designing new wells in order to increase the production rate, reduce the risk and cost, when drilling new wells in the Asmari reservoir of this oil field.

Keywords: *Seismic Data, Buried Karst, Reservoir Quality, Asmari Formation, Kupal Oil Field.*

Introduction

The information obtained by surface detectors, although precise and comprehensive, cannot provide us with all the requirements which are needed to delineate underground layers. More detailed information on the subsurface environment can be obtained by sub–surface investigations. Three dimensional seismic is one of the subsurface geophysical methods for the identification, exploration and development of oil and gas reservoirs which has been used in Iran in recent years in various hydrocarbon fields, including Kupal oil field.

The applications of seismic data in the exploration and development of hydrocarbon reservoirs are endless to count, and new methods are constantly being introduced and used in this industry. These applications have been developed because of the expansion of multi–dimensional space of seismic data as well as acquiring knowledge regarding new dimensions of data in this space, followed by the invention of new computational methods for envisaging a geological concept for these dimensions. These computational methods are referred to as seismic attributes in geophysics. The seismic attribute can be defined as assigning a quality to any criterion; and aims to provide accurate and detailed information on the interpretation of structural, stratigraphic and lithological parameters in seismic exploration (Oyeyem & Aizebeokhai, 2015).

Geological features are naturally different from the surrounding areas, affect the quality of seismic data, and provide a different seismic response, in which seismic attribute plays an important role in increasing the correctness and accuracy of displaying these features (Raef *et al*., 2015). The use of seismic attributes for detecting the buried channels by Marfurt & Liu (2007), concealed karsts (karsts hole) by Cunnell *et al.* (2013), fault–controlled karsts by Qi *et al.* (2014), imaging of karst in the Persian Gulf by M. Burberry *et al.* (2016), buried karsts in carbonate platforms by Jamaludin *et al.* (2017), as well as karsts generated in deep earth (Hypogenic Karsts) by Zhou *et al.* (2017), has been proven.

These attributes, are also widely used in detecting reef edges (Skirius *et al.* ,1999), channels filled with porous rocks (Cao *et al.,* 2015), reservoir characteristics and pay zones (Oyeyem & Aizebeokhai ,2015; Aneez ,2013) , porosity (Hosseini *et al.* 2011) and compaction (Chopra & Marfurt, 2012), geomorphology (Koson *et al.,* 2014), discontinuity of sedimentary layers, disconformities, lithology and sedimentary environments changes (Chopra & Marfurt, 2005:2008:2009; Shamsuddin *et* *al.,* 2017), and so on.

Spectral analysis has been employed in seismic exploration for more than two decades, and now it is a commonly used approach due to its advantages in reservoir characterization, thin–bed interpretation, and gas reservoir detection. Since its introduction, several methods of spectral decomposition have emerged including the short–time Fourier transform (Nawab & Quatieri, 1988), Wigner–Ville distribution (WVD) (Claasen & Mecklenbrauker, 1980), the wavelet transform (Daubechies, 1988; Mallat, 1989), the wavelet packet transform (Coifman & Wickerhauser, 1992), and Matching Pursuit Decomposition (MPD) (Mallat & Zhang, 1993; Chakraborty & Okaya, 1995).

Seismic data are band–limited typically within ranges from 10 to 70 Hz. This means that seismic data are rich in intermediate frequencies. As a result, a time–frequency transform that produces high resolution for all intermediate frequencies is required for processing seismic data.

The Matching Pursuit Decomposition (MPD) is one of the transform techniques that have been developed to meet the above–mentioned requirement (Mallat & Zhang, 1993; Chakraborty & Okoya, 1995). In the matching pursuit algorithm, each seismic trace is decomposed into a number of individual wavelets whose sum equals the original trace. After decomposing into wavelets, a trace can be reconstructed at a given central frequency. In this method, a set of basic functions is generated by scaling, translating, and modulating a single window function.

In this research, firstly, the interpretation of 3D seismic data was used to investigate the structure of the Kupal sub–surface anticline, and then seismic frequency decomposition (spectral decomposition) and inversion techniques were used to identify the paleo buried karsts and its reservoir quality of the mentioned features; such studies assist us with better reservoir planning as well as safer drilling.

Geological framework

Zagros mountain belt is divided into several zones based on the structural patterns and sedimentary history. From the northeast to the southwest of the study area (Central Zagros), it matches with the Balaroud and Kazeroun faults and is classified as thrusted Zagros, folded Zagros (central Zagros) and Abadan plain, respectively. Also, the central Zagros is divided, from northeast to southwest, into high Zagros, Izeh zone and Dezful Embayment (Falcon, 1974).

Dezful Embayment is a part of the central Zagros mountains and a rich oil province in southwestern Iran which has long been attractive for geologists and experts of oil companies; the results of their research works have been published in the form of several papers and reports, some of which can be mentioned as James & Wynd,1965; Falcon,1974; McQuillan,1991; Motiee,1995; Ziegler, 2001; Sepehr & Cosgrove, 2002:2004, Sherkati & Letouzey, 2004; Sherkati, 2005; Alavi, 1994:2004; Bordenave & Hegre, 2005:2010). This structural zone contains approximately 8% of world oil reservoirs (Bordenave & Hegre, 2005:2010) and 90% of the oil reserves of Iran (McQuillan, 1991). The Dezful Embayment is more stable than its adjacent areas in terms of tectonic movements; therefore, it encloses simpler folds (Falcon, 1974; Sherkati & Letouzey, 2004) (Fig. 1).

This embayment is characterized by a higher thickness of Tertiary deposits compared to the Fars and Lorestan areas and is about 3000 to 6000 meters lower than its neighboring areas (Motiee, 1995). In the formation of Dezful Embayment, basement faults of Qatar–Kazeroun, Izeh, Balarud and mountain front faults have played an effective role; to the extent that these fault zones controlled deposition, deformation and trapping of hydrocarbons (Sepehr & Cosgrove, 2002:2004).

The Kupal oil field is located 60 kilometers to the east of Ahvaz city in Khuzestan province (Fig. 1), and it is an extension of Aghajari anticline fold in the central part of Dezful Embayment and among large Iranian oil fields. The subsurface structure of the Kupal oil field neighbors Marun oil field to the southwest, Ramin oil field to the northwest and Aghajari oil field to the southeast. It lies within the latitude 10° 31' to 33° 31' and longitude 8° 49' to 27° 49' (Fig. 2), and the average height of the field is 155 m above mean sea level.

The outcrops of the Kupal anticline consist of alluvial deposits, Bakhtiari Formation and sandstone hills of Aghajari Formation (Lahbari member) as well as gently dipped sedimentary layers (maximum 12 degrees) (Fig. 3). The underground anticline of the Asmari Formation is covered by alluvial deposits, the Bakhtiari Formation and Fars group (Gachsaran, Mishan & Aghajari Fms.) and overlies the Pabdeh Formation gradually (Aghanabati, 2004).

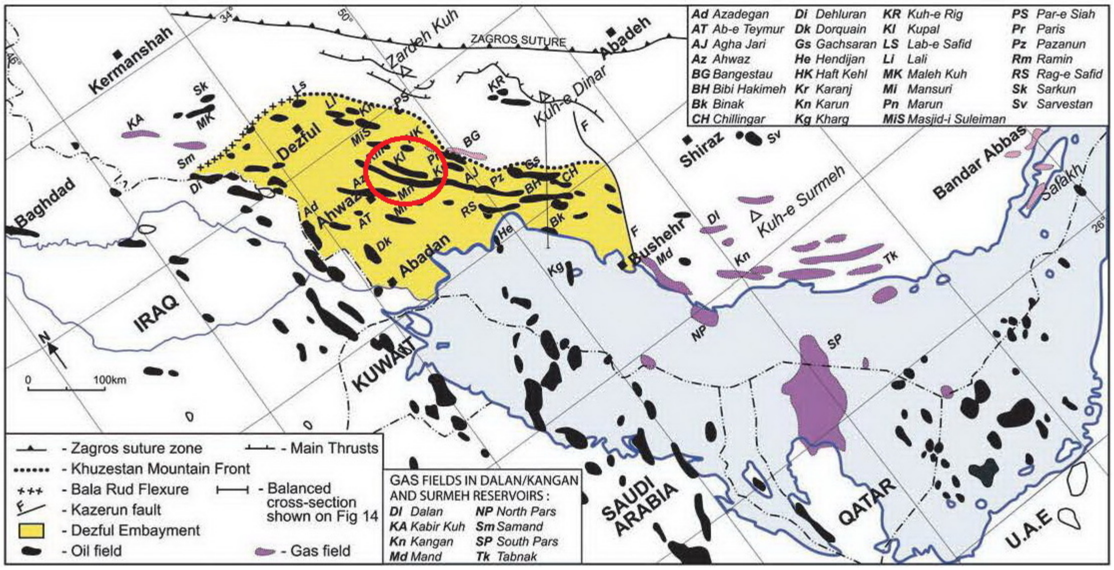

Figure 1. The geological location of Dezful Embayment (northern and southern) and the study area (adapted from Bordenave & Hegre, 2005).

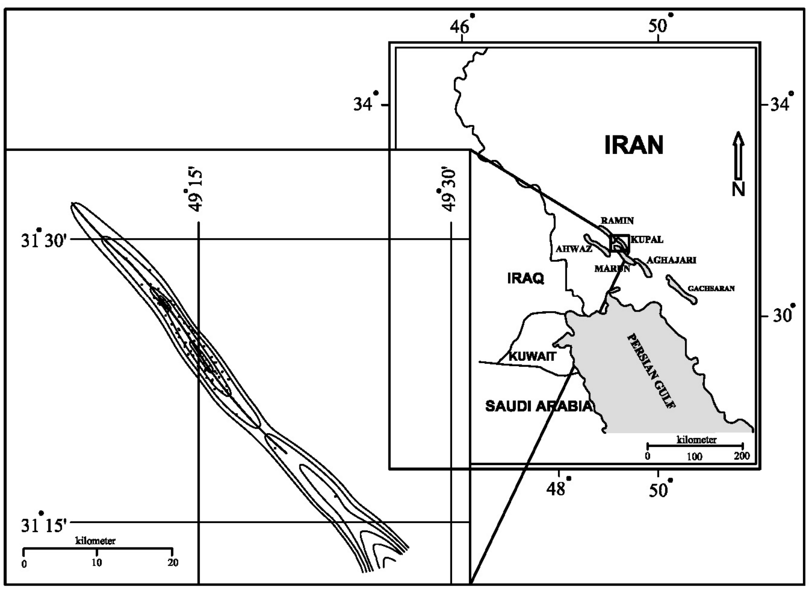

Figure 2. Geographical position of Kupal and nearby oil fields.

Asmari Formation characteristics

So far, 59 oil wells have been drilled in the Kupal oil field of which 36 wells have been completed in the Asmari reservoir. On the basis of 3D seismic data, the underground structure of this oil field is in the form of a roughly–symmetrical elongated anticline with extremely mild folding and two culminations on the Asmari horizon of the reservoir and it covers an area of 264 km^2 (60 km by 4.5 km) on this horizon.

The main culmination, into which 58 oil wells have been drilled, is located in the northwest part of the field and is referred to as the western Kupal. The smaller culmination, located in the southeastern part of the field, is known as the eastern Kupal and it is home to only one well (Well No. 2). The faults of the Kupal oil field include three thrust faults with a dip ranging from 20 to 60 degrees. The principle fault in the southwest flank has formed the main structure of the field, with its vertical displacement in various sections reaching up to 300 meters (Fig. 4).

The isodip maps on the Asmari horizon show that the structural dip on the anticline axis ranges from zero to 7 degrees and it varies from 35 degrees in the southern flank to 45 degrees in the northern flank. Based on the information acquired from the underground contour depth map of the top of Asmari horizon, the minimum depth of the reservoir crest in the western and eastern Kupal is circa 3170 and 3200 mbsl, respectively. The vertical closure of this reservoir on the western and eastern culminations, on the basis of the deepest closed contour on this horizon, is 450 and 410 m, respectively.

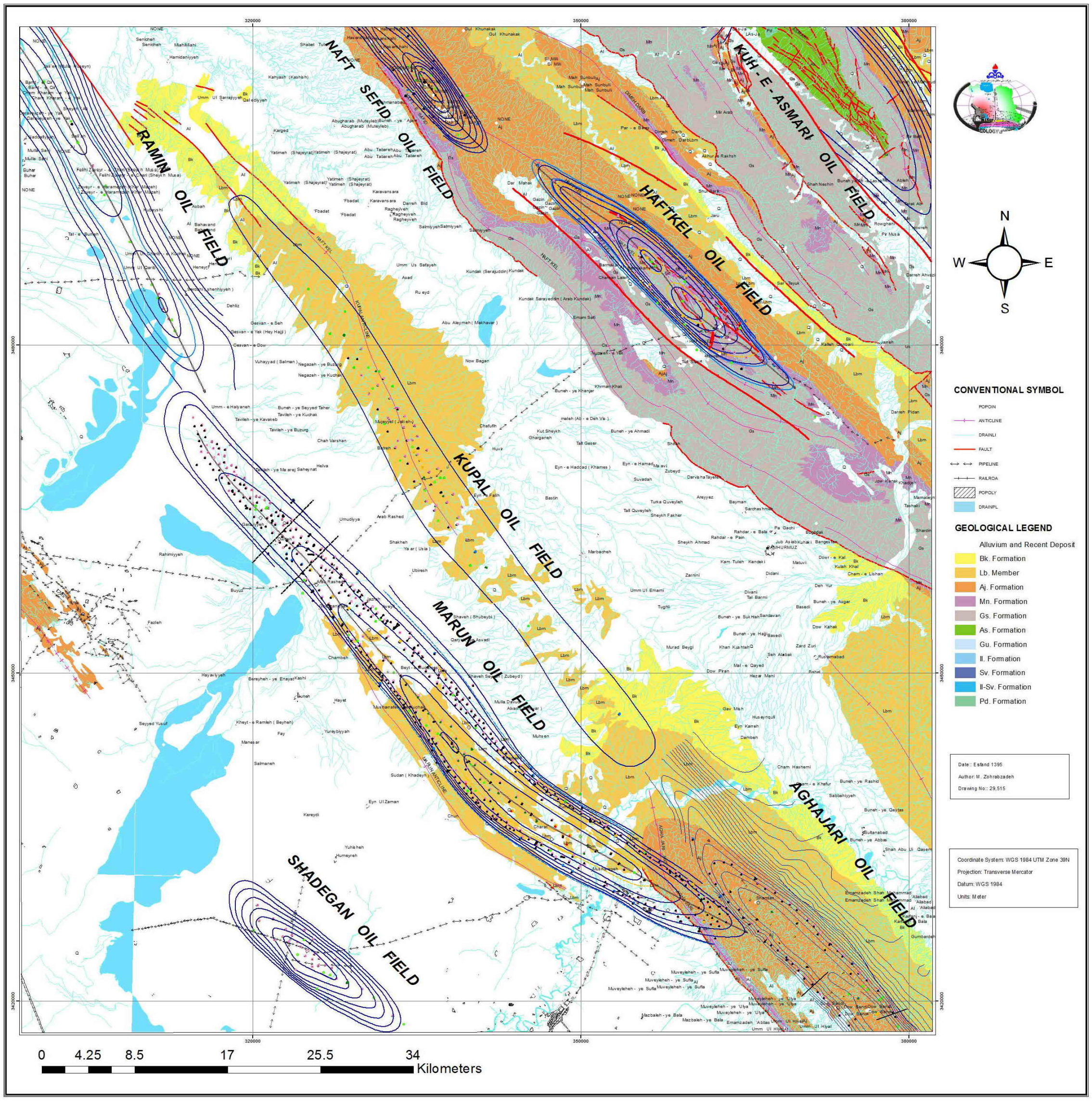

Figure 3. Geological map of the Kupal and nearby oil fields.

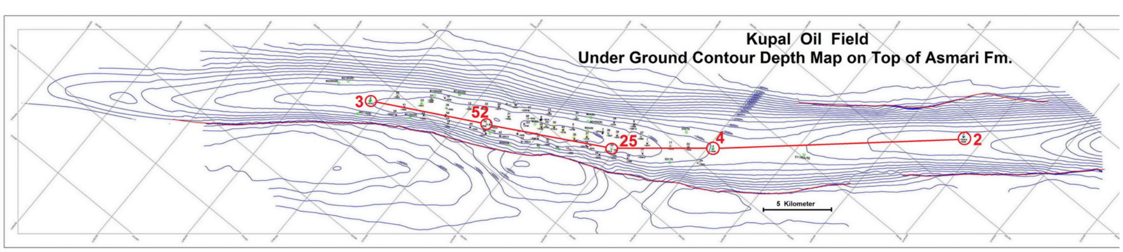

Figure 4. Underground contour depth map on top of Asmari Formation in Kupal oil field.

Lithologically, the upper two–thirds of the Asmari Formation consists of carbonates including limestone and dolomite and the remaining one third at its base comprises clastic sediments such as shale and sandstone. This formation is overlain by Gachsaran Formation with the age of the lower to middle Miocene and overlies Pabdeh Formation whose age ranges from Paleocene to Eocene (Speers, 1976), (Fig. 5).

On the basis of the data from 28 drilled wells which intruded the entire thickness of the Asmari Formation; it shows the highest thickness of 455 m in Well 57, the minimum of 390 m in Well 4 and an average thickness of 417 m as a whole. The Asmari Formation is an under–saturated reservoir with no gas cap, in which the propulsion force is produced only through the expansion of the oil and therefore it does not include active water zone. Its oil is sweet with 32–34API and contains a low amount of H_2S. The initial pressure of the reservoir was 5653 psi at a depth of 3350 mbsl and a temperature of 219 degrees Fahrenheit at the same depth. The average elevation of water–oil contact is 3597 mbsl in the western culmination. The highest initial thickness of the hydrocarbon column in this reservoir in the western culmination was about 427 meters. With an average porosity of 12% and an average water saturation of 26%, the initial in–situ volume of oil in the Asmari reservoir was estimated at about 4.75 billion barrels. This ends up to about 650 million barrels of producible oil if initial recovery rate of 13% is taken into account (Ansari & Safaee, 1986; Roghanian & Farazmand, 2008).

Data and Methods:

Seismic structural interpretation

In order to use the 3D–seismic attributes of the Asmari Formation in the Kupal oil field, first, a seismic interpretation workstation was set. The coordinate system suitable for the study area was selected as WGS 1984–UTM in the 39N zone. In the second step, processed seismic data, drilled wells data, wave velocities and the other required information were inputted into the relevant computer code and the structural interpretation of 3D seismic data was carried out. The results of the interpretation of the sub–surface structure of the Kupal oil field in the western and eastern culminations in two selected seismic profiles are shown in figures 6 and 7.

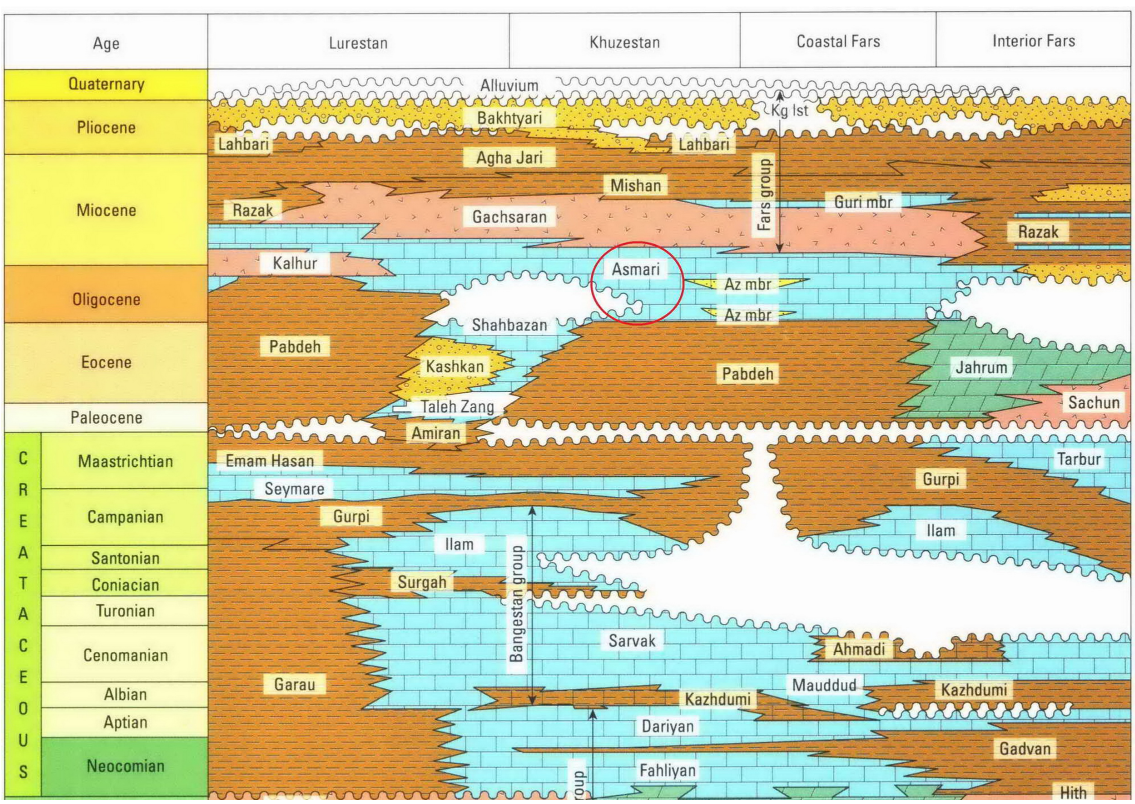

Figure 5. A schematic chronostratigraphic section of Khuzestan, Lorestan and Fars provinces from Cretaceous till the present time (adapted from James & Wynd, 1965).

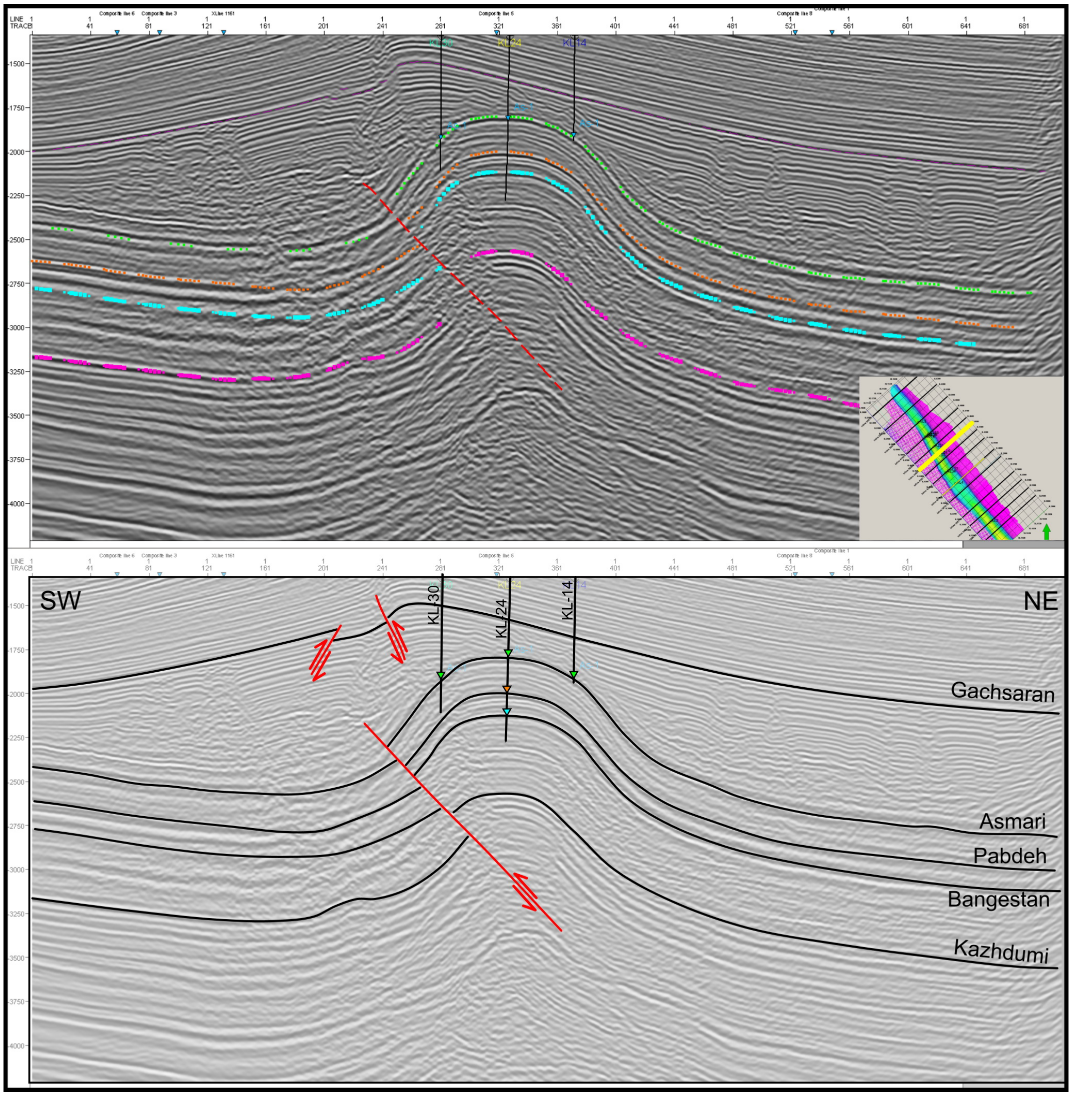

Figure 6. Seismic cross-axial profile in the western culmination of Kupal anticline which passes through wells no. 14, 24, and 30.

The activity of the thrusted faults in the northern and southern flanks can be clearly seen.

Seismic cross–axial profile of the western culmination of the Kupal anticline:

This profile passes through wells no. 24, 14 and 30 (Fig. 6). The Kupal anticline shows harmonic structure (from Asmari to Jurassic) and a symmetrical cylindrical fold in the area around these wells. Based on the second–derivative seismic attribute, the dip in the northern flank is about 35 degrees and in the southern flank it is estimated at 29 degrees. The anticline in this area has generated the main culmination of the Kupal structure. The southwest flank of thrust fault has led to a large displacement of about 300 m in the Bangestan horizon. The folding model in this section of the field is also consistent with the fault propagation fold (Sherkati *et al.,* 2005; McClay *et al.,* 2011). The assessment of thickness variations along the anticline and its isodip contours shows that the type of anticline in the Asmari and Bangestan horizons to Khami group based on the Ramsey classification (Ramsay & Huber, 1987) is 1B. In other words, the actual thickness of the reservoir horizons in the anticline axis and its flanks is approximately identical.

Seismic cross–axial profile of the eastern culmination of Kupal anticline:

This profile passes through Well no. 2 and is perpendicular to the anticline axis (Fig. 7). The Kupal anticline shows inharmonic structure (from Asmari to Jurassic) and an asymmetrical cylindrical fold around this well. Based on the second derivative seismic attribute, the dip of the northeast flank is 35 degrees and that of the southwest flank is 37 degrees. In this part of the field, increasing tension compared to its nose and reduction of space in the anticline core has led to the occurrence of at least three thrust faults in both flanks, showing a vertical displacement of 100 to 300 m in Asmari and Bangestan horizons. Due to the activity of this fault, the anticline has been reformed to a Transported Fault Propagation Fold (Sherkati & Letouzay, 2004). Also, there are signs of inactivation of this fault and generation of a back trust in the northeastern flank and in the possibly–Jurassic horizon. In this profile, thickness changes along the anticline and its isodip contours indicate that the type of anticline in the Asmari and Bangestan horizons to the Khami group based on the Ramsey classification (Ramsay & Huber, 1987) is 1C.

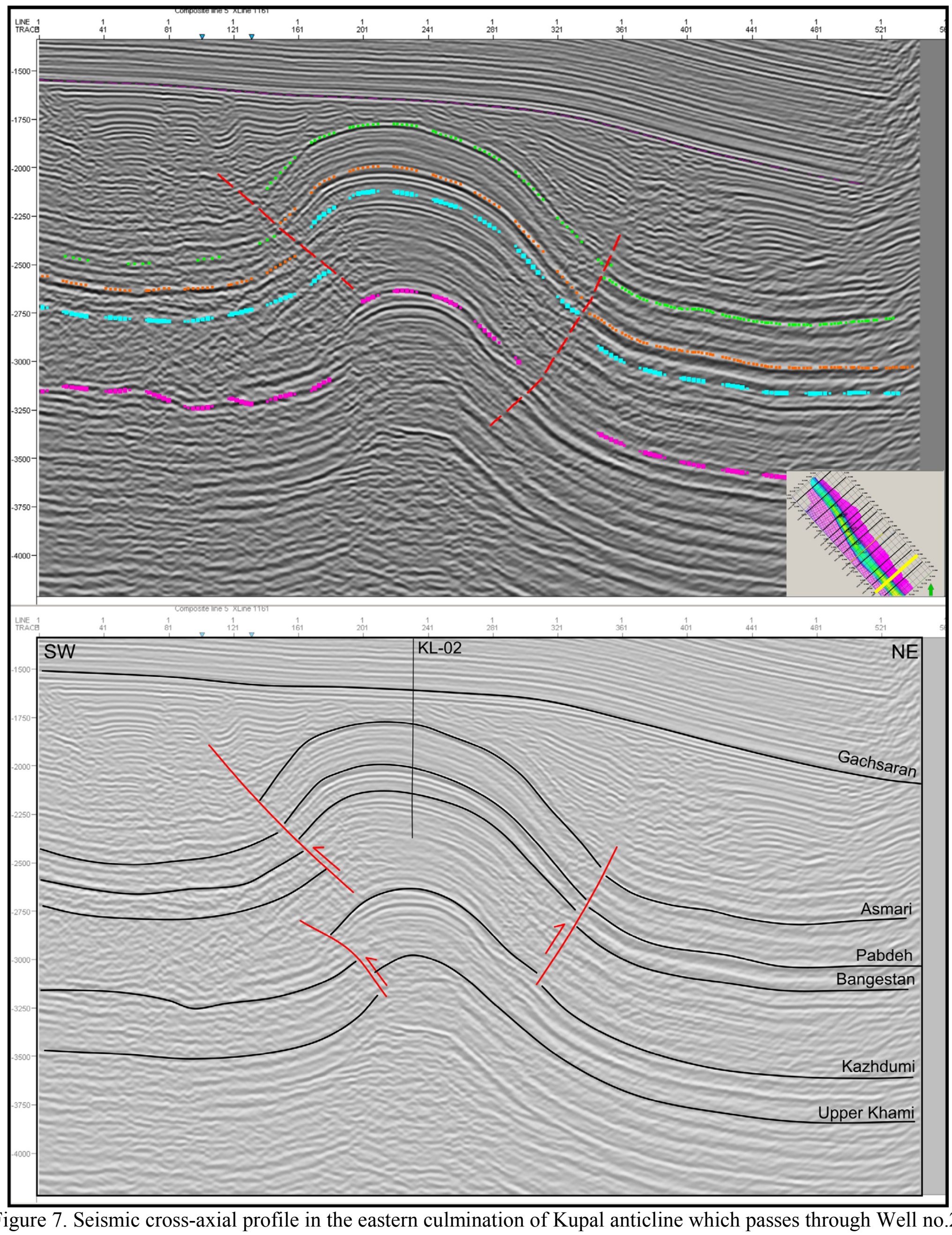

Figure 7. Seismic cross-axial profile in the eastern culmination of Kupal anticline which passes through Well no.2.

Use of seismic attributes

Since the Earth acts as a low pass filter during seismic waves propagation (It filters the high frequencies), it changes the frequency bandwidth of seismic waves with time; therefore, the conventional methods of seismic data display, despite their extensive applications, cannot simultaneously display both time and frequency data in a dedicated manner. The simultaneous use of such large amount of data is troublesome both computationally and in terms of interpretation; therefore, methods that can reduce this large amount of data and, at the same time, do not invalidate the existing information, are highly valuable (Liu & Marfurt, 2007).

By using 3D seismic frequency decomposition technique, those geological features that are not within the seismic amplitude resolution range are detected; then in the next step, by the help of spectral decomposition, these geological features can be combined together in the best possible arrangement (Liu & Marfurt, 2007). To do this, the data from spectral analysis were first decomposed into cubes of frequency–time and the recognized geological patterns in the seismic data were studied for each cube. Finally, seismic frequency decomposition data were used for detecting and exploring buried karsts features.

On the other hand, by using seismic structural interpretation, a cube of seismic amplitude data in the study area of the reservoir was cropped. These cubes, which contain useful information about structural trends and sedimentary deposits, are used to illustrate geological features (Fig. 8). Next, the data range was transferred from seismic amplitude to seismic frequency, and a cube containing the tuning phenomenon was extracted from the conventional 3D seismic data.

A seismic profile contains a large range of different frequencies of the seismic wave which is called frequency bandwidth. In figure 9, the frequency bandwidth of a seismic cross section is considered at several different sections in constant frequency intervals. Since, low and high frequencies each include separate information about geological events, single–frequency images cannot display the required information from geological events simultaneously; therefore, the adjacent sections that cover a range of frequency data are combined with the dominant frequency of blue, green, or red colors (based on seismic interpreter experience and seismic slice frequency bandwidth), and eventually the resulting color frequency sections are merged and form a RGB colored spectrum slice. This process is called Blended Frequency Decomposition (Liu & Marfurt, 2007), (Fig. 9).

These frequency ranges will vary according to the geophysicist's experience and whether the objective is to look for large fractures (high frequencies) or buried channels (low frequencies). Finally, the RGB cube is cut along the required horizons; it is then examined and used to better identify the buried channels and large fractures that can be a good place to accommodate hydrocarbons. Subsequently, the interpretation of the structural 3D seismic data of Asmari and Pabdeh horizons were entered into the frequency cubes. These horizons have been used as the basis for measuring the variation of the seismic spectrum in this field, and, slices parallel to the top of Asmari Formation in the upper, middle and lower parts of Asmari in the final frequency spectrum cubes have been prepared and analyzed (Fig. 10)

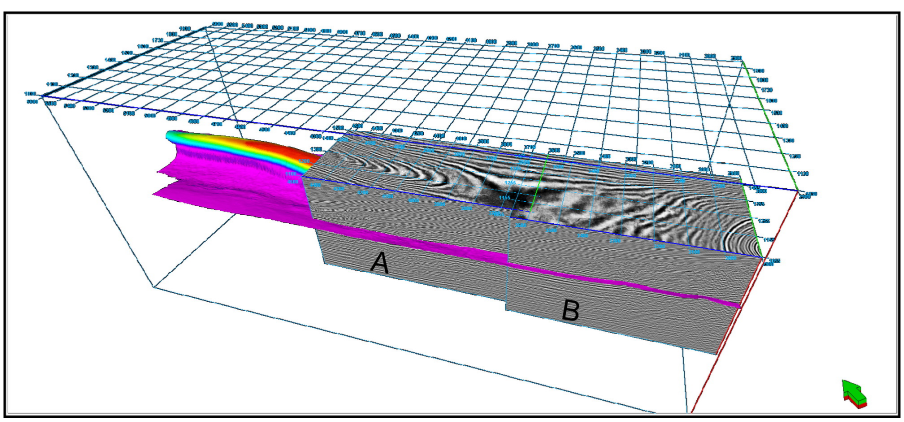

Figure 8. Cubes cropped from 3D seismic data in the Asmari Formation of Kupal oil field

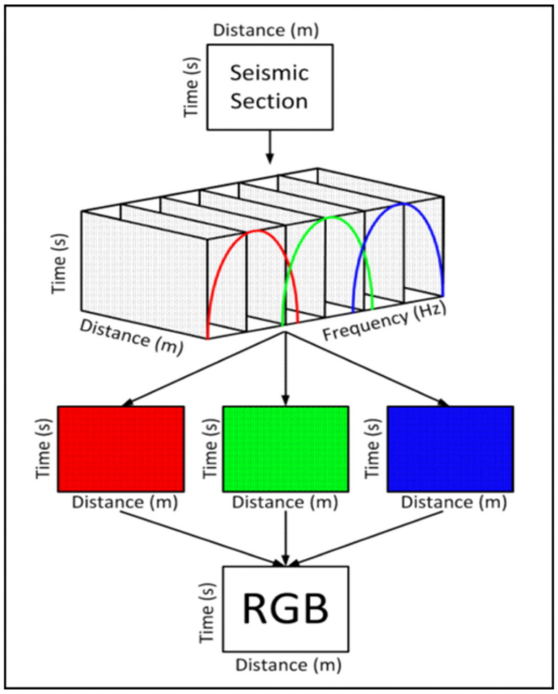

Figure 9. The method for generating RGB colored spectral images (Revised after Liu & Marfurt, 2007).

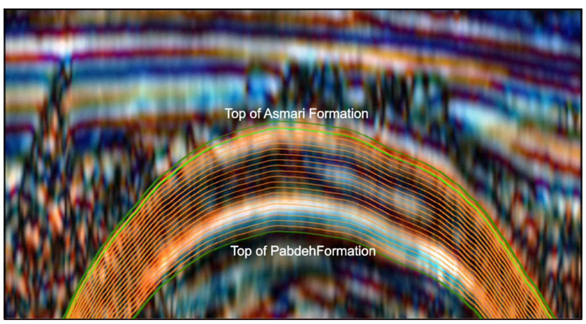

Figure 10. An example of parallel cutting planes in spectral decomposition cubes in an interval between the Asmari and Pabdeh horizons in the Kupal oil field, in which the parallelism between the upper and lower parts of the formation has been followed.

Analysis of the frequency data at the top of Asmari Formation of the Kupal oil field by the help of multiple color spectrum compositions strongly points to the existence of buried karstic features (mainly as channels) in this horizon. In the final color combination, at least 7 karstic trends are detectable; A–B–C karsts lie in the western Kupal and D–E–F–G karsts are located in the eastern Kupal (Fig. 11).

Geophysical studies have shown that these trends are mainly seen in the upper 30 m of the Asmari Formation of the Kupal oil field and gradually disappear at depth. It is necessary to note that the footpath of the observed karstic processes does not cross any of the drilled wells sites in the Asmari Formation of the Kupal oil field. In order to ensure that these karstic features (channels) are real, the effects of these phenomena on the seismic acoustic impedance needed to be investigated. For this purpose, the results of the inversion of the three–dimensional seismic data of Asmari Formation have been used.

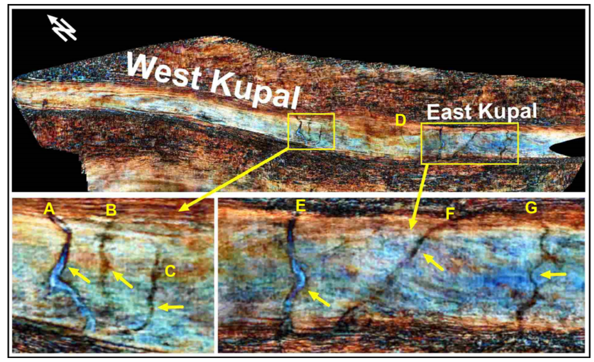

Figure 11. (Top) Spectral decomposition attribute for 30 m below the top of Asmari Formation of Kupal oil field, (Bottom) Two main areas with buried karstic trends.

Our investigations showed that the effect of karstic features is clearly visible to depths approximately 30 m below the top of Asmari Formation in horizontal seismic acoustic impedance maps. For example, in figure 12, the acoustic impedance horizontal section of the karstic features no. E with an average width of 200 m related to a depth of 30 m below the Asmari Formation in the East Kupal is illustrated.

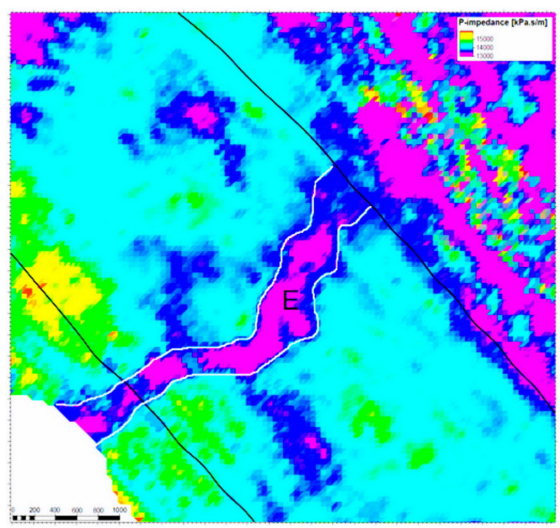

Figure 12. Horizontal section of seismic acoustic impedance of 30 m below the top of Asmari Formation & trend of karst no. E in the eastern culmination of Kupal anticline.

As shown, this karstic features possesses lower seismic acoustic impedance than the surrounding area. Thus, because of having higher effective porosity, it has a better reservoir quality. Therefore, when drilling for new wells, the position and characteristics of the relevant karstic features should be considered (Chen & Sidney, 1997; Fahmy *et al.,* 2005).

Geological Data

The results of cores analysis in the upper part of the Asmari Formation including wells No.2, 4, 6, and 44, shows that the carbonate facies have a porosity which ranges from 2.5 to 20% and a permeability of 0.05 to 100 millidarcy (Nasiri & Ehsani, 2014). However, the statistical calculations derived from seismic data modeling show that the permeability in the karstic intervals has increased to 1,000 millidarcys. Solution features are diverse in size, ranging from microscopic to macroscopic.

The karstification phenomenon and relevant geomorphological features are the result of water reacting with calcareous and other dissolvable rocks. Karstic areas develop special geomorphic features either at the surface or subsurface, and the patterns of the features created by the water flows are generally controlled by secondary porosity. Buried karst phenomena were created at or near a former land surface by the action of meteoric waters and developed before the cover strata were laid down (Bosak *et al.,* 1989). The karrens, grikes, sinkholes or dolines, sinking streams, caves, springs, channels, and karstic valleys (karstic canyons) are examples of karstic landforms (Ford & Williams, 2007). In the Kupal oil field, this large scale dissolution features have dimensions between 10 to 200 m in width and depths of 5 to 30 m. They appear as spring shape, channels and even valley.

Paleokarsts are formed during periods of sea–level low–stands or uplift and subaerial exposure of carbonate platforms.

Following sea water transgression, these features are generally covered by shale or evaporate sediments and consequently sealed porous horizons are developed. Similar features are reported from various carbonate reservoirs such as boundary of the Kangan and Dalan formations (e.g., Rahimpour–Bonab, *et al.,* 2009; Esrafili–Dizaji & Rahimpour–Bonab, 2013), in the Cenomanian – Turonian and Early Turonian of the Sarvak Formation (Ashrafzadeh, 1999; Rahimpour–Bonab *et al.,* 2012 & 2013). Avarjani (Avarjani *et al.,* 2014) refers to the presence of the paleokarsts in the drill cores of the upper Asmari in the Marun oil field (Fig. 13).

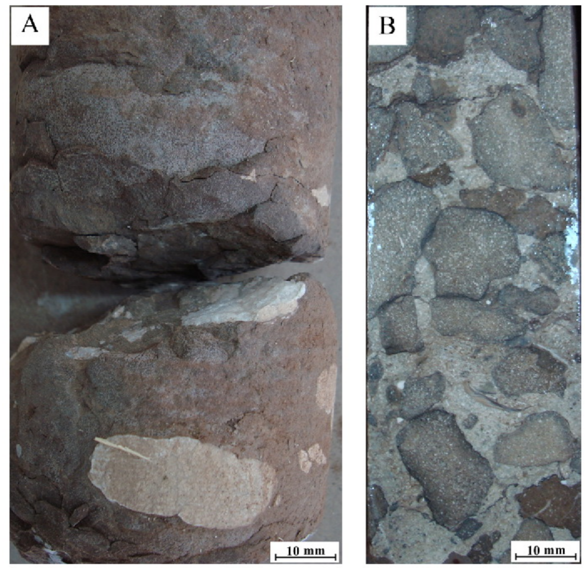

Figure 13. The effects of karstification on the upper Asmari limestone in Marun oil field cores (A) karstification with iron oxide in limestone (B) Paleokarst (Avarjani *et al*., 2014).

According to this research, they are present at the top of Asmari Formation (lower Miocene).

The upper part of Asmari Formation in Kupal oil field is deposited in the High Stand System Tract (HST) and Forced Regressive System Tract (FRST) (Omidpour *et al,* 2006; Avarjani *et al.,* 2011). Finally, by the sea level regression, the evaporitic sediments of the Gachsaran Formation have been deposited (Fig. 14). According to Amini (2005 & 2009) and other researchers (e.g., Rahimpour–Bonab *et al.,* 2013; Mehrabi *et al.,* 2018), at the end of HST and FRST system tracts and under the low stand system tract (LST) palaeosol and karstic features could be formed.

In order to study the lithological characteristics of the upper Asmari in the Kupal oil field, from the northwest to the southeast of the field, the stratigraphic correlation chart was prepared for wells Nos. 3, 52, 25, 4, and 2.; the petrophysical data of the wells is displayed on such chart (Fig 15). As shown, the Asmari Formation is covered by evaporite sediments of the Gachsaran Formation.

The upper part of Asmari Formation is mainly composed of carbonate deposits (limestone and dolomite) and there are no traces of clastic sediments up to 55 meters below this horizon.

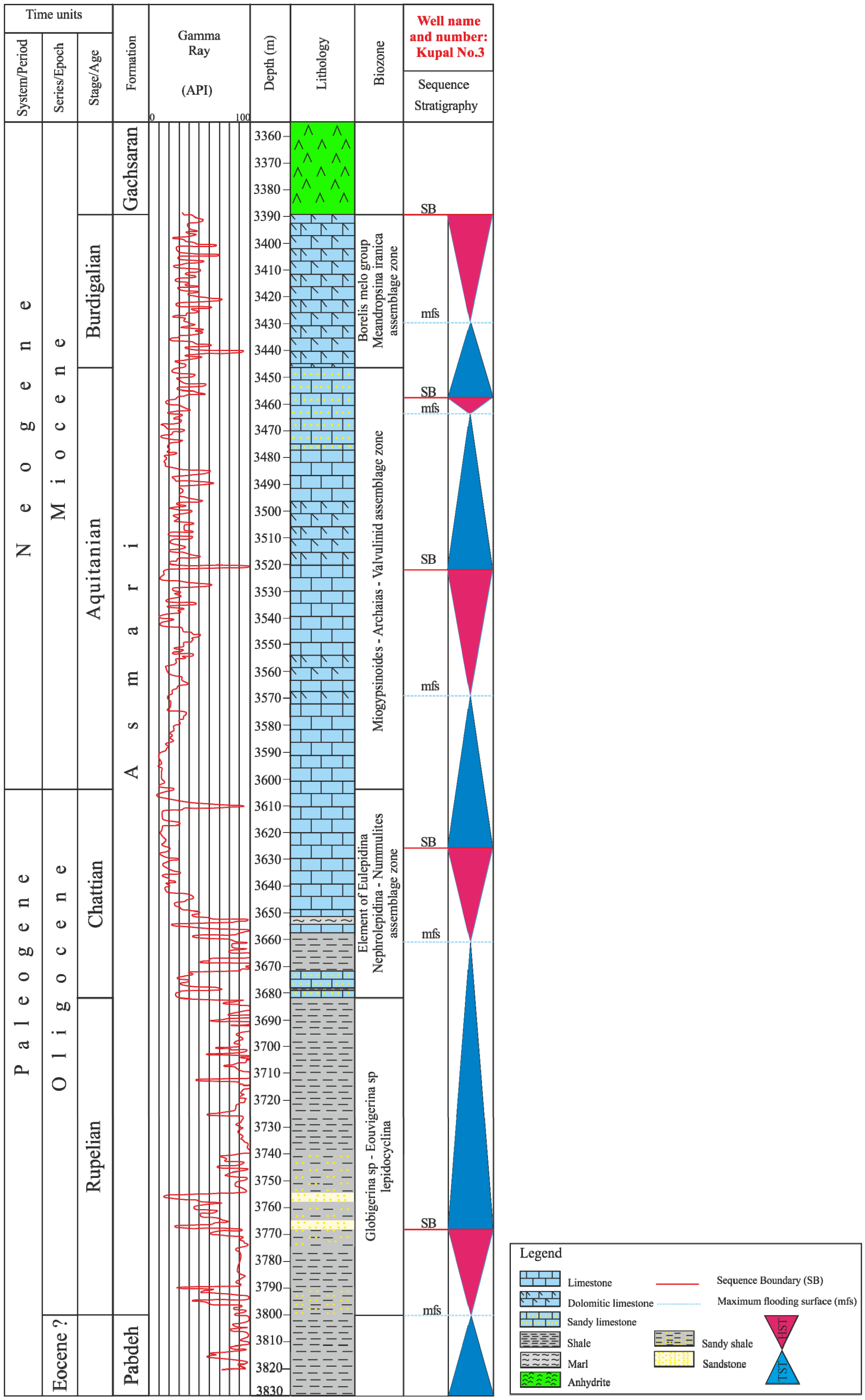

Figure 14. The stratigraphic column of Asmari Formation of the Kupal oil field in well no.3, which shows the stratigraphic sequences and biozones.

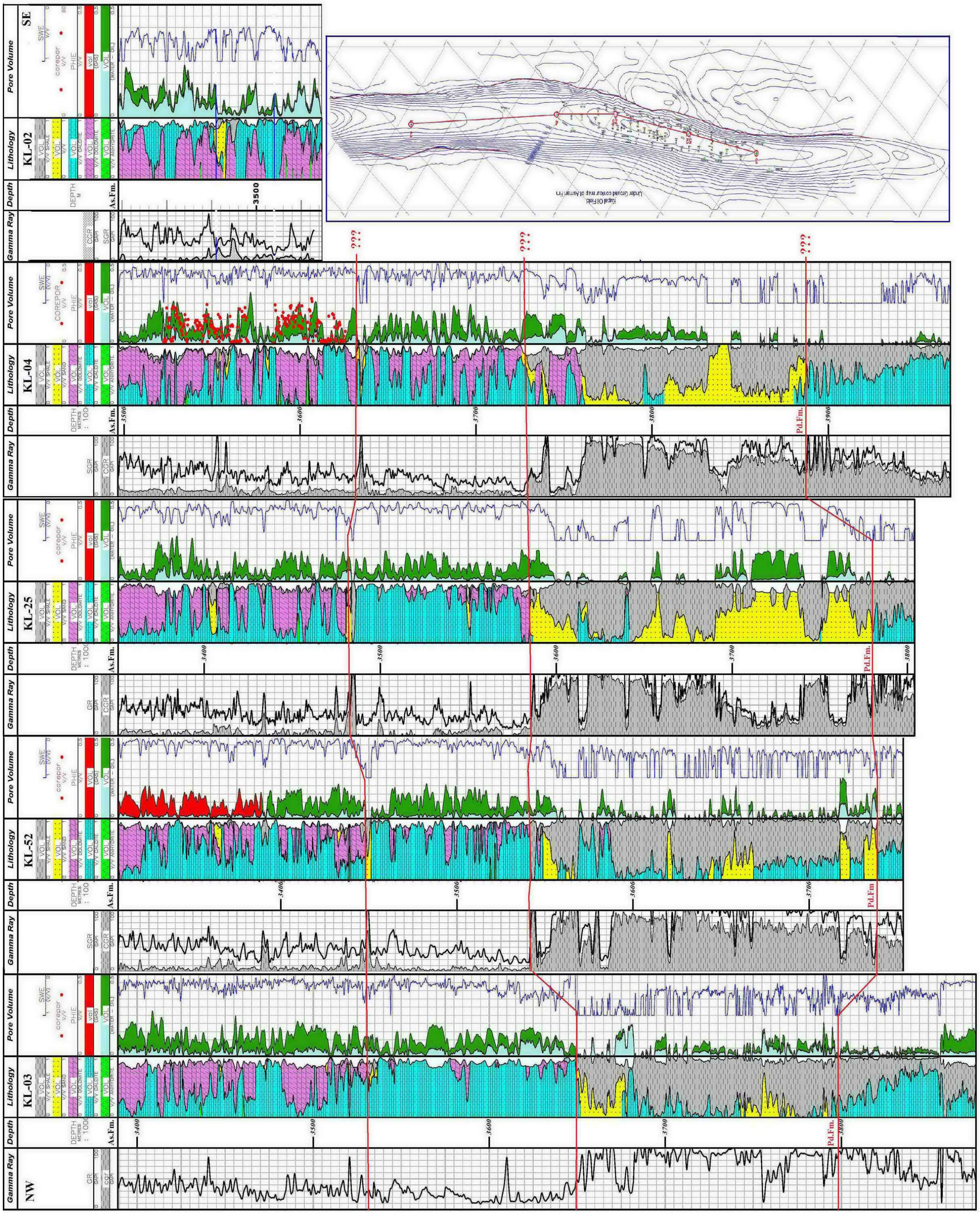

Figure 15. The stratigraphic correlation chart of Asmari Formation of the Kupal oil field, which passes through wells no. 3, 52, 25, 4, and 2.

The presence of the karstic features which are seen in three–dimensional seismic data, indicates the period of subaerial exposure resulted in the extensive dissolution of these limestones along the specified trends. The occurrence of some karstic features such as fenestrate, vuggy and extended vuggy porosities, which are sometimes plugged by sabkhas anhydrite, as well as other evidences of tidal and supratidal environments in the upper parts of the Asmari formation, and at the boundary between this unit and the Gachsaran Formation, all confirm period of the subaerial exposure.

In this part of the Asmari Formation, in the Kupal oil field, two evaporite–carbonate and mudstone/dolomudstone facies are seen. The presence of anhydrite as evaporative facies, along with the upper Asmari carbonate facies, has resulted in the formation of mixed evaporate–carbonate facies at the highest part of the Asmari Formation of the Kupal oil field (Fig. 16– A and B).

Also, the presence of fenestrate fabrics in the mudstone/dolomudstone facies could be due to the dissolution of anhydrite or unstable calcareous minerals (Parham *et al.,* 2010; Aleali *et al.,* 2013), (Fig. 16–C).

The lack of fossils and presence of anhydrite nodules as well as fenestrate fabrics all indicate that these facies are formed in the upper parts of the tidal flat zone (supratidal) in arid climates under meteoric conditions (Tucker, 1991; Shinn, 1983; Jahnert & Collins, 2012). Expansion of dissolution phenomenon leads to the development of dissolution porosities (Fig. 16–D), and finally, the continuation of these conditions resulted in karst development. In figure 17, the effects of dissolution features, such as vuggy porosity, anhydrite nodules and breccias rocks (Farsimadan, 2015) in the upper part of the Asmari Formation, are shown in the well No.52 of the Kupal oil Field. In the studied field, considering geomorphology of the karstic features and seismic interpretations, it seems that the flow direction of subsurface waters during karstification in the top of the Asmari Formation was from the northeast to the southwest.

Discussion

In various carbonate reservoirs of the southwestern Iran, fracture porosity and enlarged dissolution porosities, formed by karstification, are very important for the increase of hydrocarbons production, and this study is conducted to shed light on this issue.

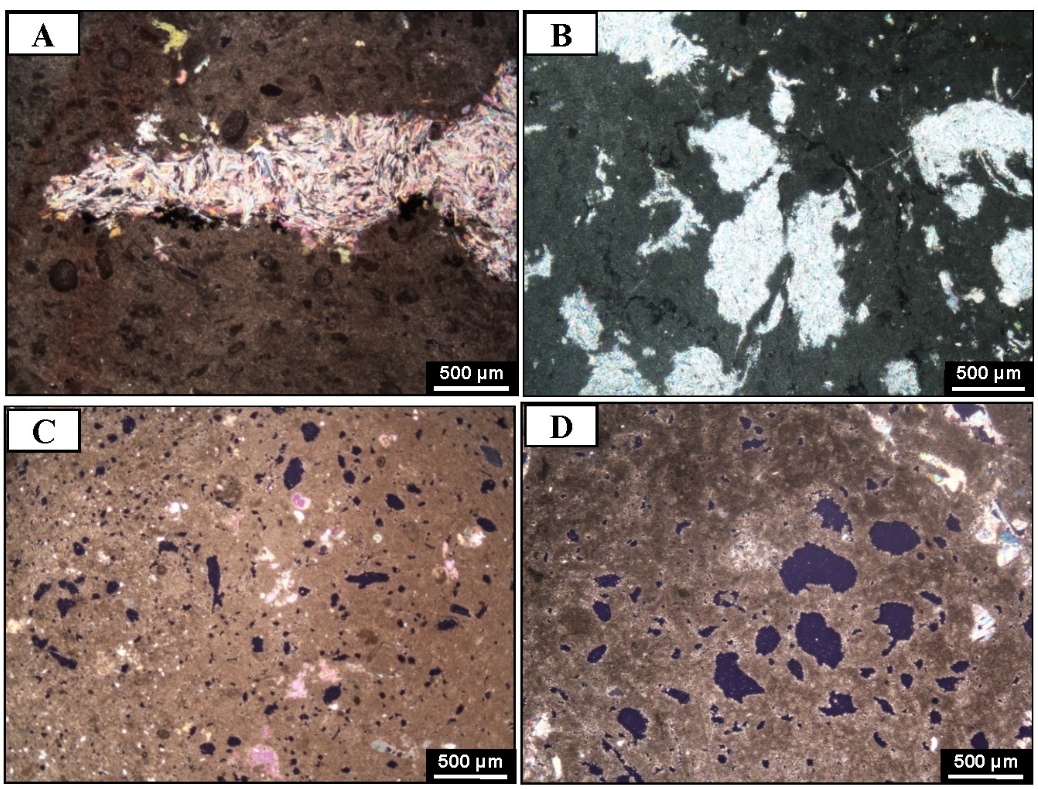

Figure 16. Microscopic images of mudstone/dolomudstone carbonate facies in the Asmari Formation of Kupal oil field (A) Anhydrite as nodules patches in carbonate facies (Kl # 4, Depth = 3518 m) (B) Anhydrite dispersed in the carbonate facies (Kl # 6, Depth = 3330 m) (C) Fenestral porosity in carbonate facies (Kl # 4, Depth = 3535 m) (D) Vuggy & extended vuggy porosity in the carbonate facies (Kl # 4, Depth = 3540 m).

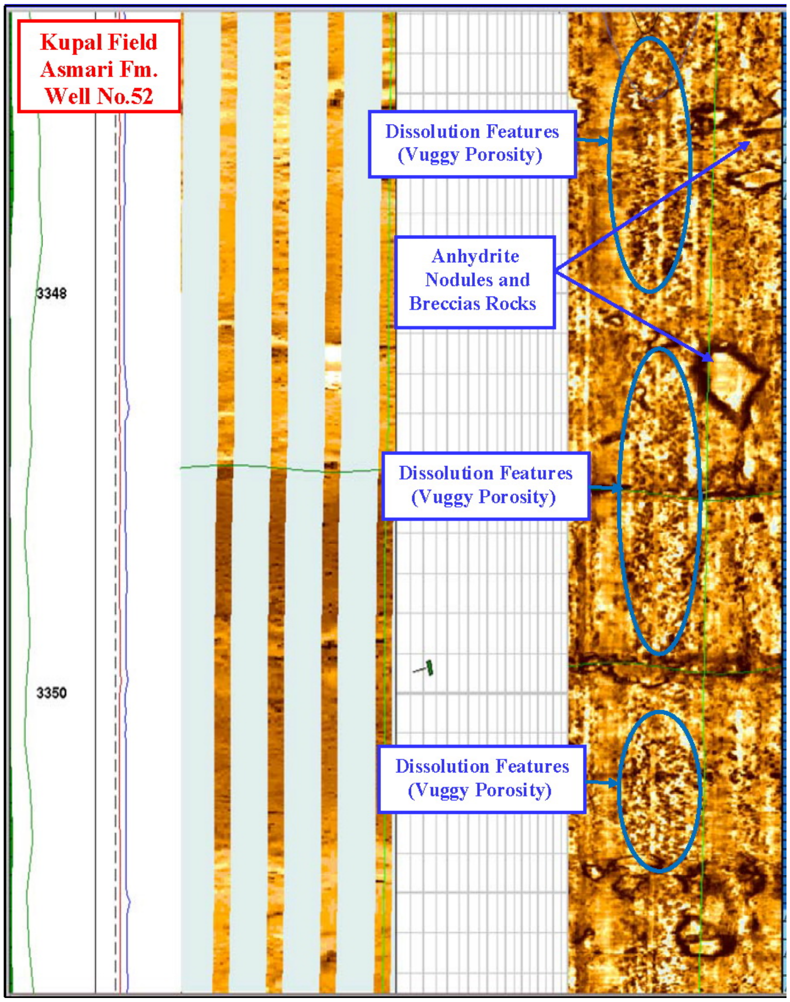

Figure 17. An example of dissolution features and related patterns on the image log at the upper part of Asmari Formation, Well No. 52, Kupal Oil field.

Also, previous bitter experiences including loss of life and property due to oil wells eruption during drilling in the karstic intervals all points to the importance of studying buried karsts. The most prominent examples of drilling fluid complete loss in the buried karsts at the top of Asmari Formation are seen in the Rag–e–Safid (Wells no. 2, 3, 33, 120 and 147) , Bibi Hakimeh (Well no. 76), Ahvaz (Wells no. 6 and 101), Aghajari (Well no. 131) and Masjid–i–Soleiman (Well no. 311) oil fields (Ghorbani, 2014). Hence, in this research, seismic technique, specially 3D seismic data, was used to study buried karsts. For this purpose, 3D–seismic data, drill core analysis (in 4 wells), drill cuttings, microscopic thin sections, petrophysical evaluations, wells completion reports (in 56 wells) and image logs (in 6 wells) (Fig. 17) in the upper part of Asmari Formation in Kupal oil field were investigated.

Through the study of seismic decomposition attribute, karstic features were identified in the eastern and western culminations of the field and after that, the seismic inversion technique showed that the relevant trends enclose considerable porosity and permeability. However, so far no wells have been drilled in these karstic intervals.

The petrographical study of drill cores and drilling cuttings shows that the existence of tidal flat and supratidal facies in the upper part of Asmari Formation which contain dissolution features, indicating suitable conditions for karst features formation in the upper part of this unit.

Conclusions

This research shows the efficiency of simultaneous use of seismic frequency decomposition and inversion seismic techniques for detecting and describing karstic features in the Asmari Formation of the Kupal oil field. The relevant trends are seen in the upper 30 meters of carbonate rocks of this formation and disappear gradually at depth. The karstic features have lower seismic acoustic impedance and higher effective porosity than the surrounding rocks and follow northeast–southwest direction. Geological investigations show that these karstic interval in carbonaceous rocks of the Asmari Formation are most likely due to the period of subaerial exposure and dissolution of the upper limestone of this unit. Severe loss of drilling fluid also supports this issue.

The results of this research can greatly help to increase the production of the Asmari reservoir in the Kupal oil field. The location and reservoir quality of these karstic features should be considered in drilling new wells to improve of production and reduce both risk and cost of drilling.

Acknowledgment

The authors thank the National Iranian South Oil Company for providing geophysical data, core samples and microscopic thin sections. They also appreciate Islamic Azad University (Science and Research Branch) for logistic support during this study. We also acknowledge Editor–in–Chief of Geopersia journal and anonymous reviewers for their reviews and suggestions that improved this manuscript significantly.

References

Aghanabati, A., 2004. The Geology of Iran, Geological Survey of Iran pub., 586: 17–34, 236–240, 289–303 (in Persian)

Alavi, M., 2004. Regional stratigraphy of the Zagros folded–thrust belt of Iran and its Proforeland evolution, American Journal of Science, 304: 1–20.

Alavi, M., 1994. Tectonic of Zagros Orogenic belt of Iran: new data and interpretations, Tectonophysics, 239: 211–238.

Amini, A., 2009. Fundamental of sequence stratigraphic, University of Tehran pub., 324: 147–160 (in Persian)

Amini, A., 2005. Significant of FRST and LST discrimination in sequence stratigraphic studies, Examples of Asmari and Qum Fm., Earth science symposium, Iran, Tehran, 8: 1–8 (in Persian)

Anees, M., 2013. Seismic attribute analysis for reservoir characterization, 10th Biennial international conference & exposition, Department of earth sciences; IIT Bombay, Mumbai , P–119, 4: 1–4

Ansari, A., Safaee, J., 1986. Assessment of performance and computation of in situ oil reserve of Asmari reservoir: Kupal oil Field, National Iranian South Oil Co., Report No. P–3987, 80: 1–80 (in Persian)

Ashrafzadeh, A., 1999. The Role and Importance of Paleohigh in South Dezful Region , Southwest Iran, NIOC, Exploration Directorate ,Tehran ,Iran, GR–1919, 63: 1–63. (In Persian)

Avarjani, S., Mahboubi, A., Moussavi–Harami, R., Amiri–Bakhtiar, H., Brenner, R.L., 2014. Facies, Depositional sequences, and Biostratigraphy of the Oligo–Miocene Asmari Formation in Marun oil field, North Dezful Embayment, Zagros Basin, SW Iran , Science Direct , Elsevier pub., PALWOR–299. 23: 15–18.

Avarjani, S., Mahboubi, A., Moussavi–Harami R., 2011. Microfacies, Sedimentary environments & Sequence Stratigraphy of Asmari Fm. in the Kupal oil field, Earth Science Journal, No.19, 16: 45–60 (in Persian).

Bordenave, M.L., Hegre, J. A., 2010. Current distribution of oil and gas fields in the Zagros fold Belt of Iran and contiguous offshore as the result of the petroleum systems. In: P. Leturmy, and C. Robin, (Eds.), Tectonic and stratigraphic evolution of Zagros and Makran during the Mesozoic–Cenozoic, Geological Society, London, Special Publications, 330: 291–353.

Bordenave, M.L., Hegre, J.A., 2005. The influence of tectonics on the entrapment of oil in the Dezful Embayment, Zagros fold belt, Iran, Journal of Petroleum Geology, 28(4): 339 – 368.

Bosak, P., Ford, D.C., Glazek, J., Horasek, I., 1989. Paleokarst: a systematic and regional review, Elsevier pub. Amsterdam – Oxford – New York – Tokyo, 685: 19–34.

Burberry, M., Jackson, CA–L., Chandler, S., 2016. Seismic reflection imaging of karst in the Persian Gulf; Implications for the characterization of carbonate reservoirs, AAPG Bulletin, DOI: 10.1306/04151615115, ISSN: 0149-1423, 43: 1–43

Cao, J., Yue, Y., Zhang, K., Yang, J., Zhang, X., 2015. Subsurface channel detection using color blending of seismic attribute volumes, International Journal of Signal Processing, Image Processing and Pattern Recognition, Vol.8, No.12, pp.157–170 http://dx.doi.org/10.14257/ijsip.2015.8.12.16, 14: 1–14

Chakraborty, A., Okaya, D., 1995. Frequency–time decomposition of seismic data using wavelet–based methods. Geophysics, 60: 1906–1916.

Chen, Q., Sidney, S., 1997. Seismic attribute technology for reservoir forecasting and monitoring: The Leading Edge, 16: 445–456.

Chopra, S., Marfurt, K. J., 2012. Seismic attribute expression of differential compaction, SEG Las Vegas, Annual Meeting, http://dx.doi.org/10.1190/segam2012–1323.1, 5: 1–5

Chopra, S., Marfurt, K. J., 2009. Detecting stratigraphic features via cross plotting of seismic discontinuity attributes and

their volume visualization, The Leading Edge pub., http://segdl.org, 5: 1–5.
Chopra, S., Marfurt, K. J., 2008. Seismic attributes for stratigraphic feature characterization, AAPG, Search and Discovery Article#90170©2013 CSPG/CSEG/CWLS Geo Convention, Calgary, Alberta, Canada, 4: 12–15
Chopra, S., Marfurt, K. J., 2005. 75th Anniversary seismic attributes –A historical perspective: Geophysics , 70 (5): 3–28, 32 FIGS. Edge, 15:1090**.**
Classen, T., Macklenbrauker, W., 1980. The Wigner distribution – A tool for time–frequency signal analysis (3 parts). Philips J. Res, 35: 217–250, 276–300, 372–389.
Coifman, R.R., Wickerhauser, M.V., 1992. Entropy–based algorithms for best basis selection. IEEE Trans. Inf. Th., 38: 713–719.
Cunnell, C., Adel, E.E., Adel, Eb., Wael, Z., Badr, A.A., Tamer, S., Andreas, L., Refat, S., Hossam, A.W., 2013. Delineation of karst, a new approach using seismic attribute–Case study from Kuwait, SEG Houston Annual meeting, 4: 3846–3850.
Daubechies, I., 1988. Orthonormal bases of compactly supported wavelets. Comm. in Pure Applied Math, 41: 909–996.
Esrafili–Dizaji, B., Rahimpour–Bonab, H., 2013. A review of Permo–Triassic reservoir rocks in the Zagros area, SW Iran: influence of the Qatar–Fars arch. Journal of Petroleum Geology, 36 (3): 257–279.
Fahmy, W. A., Matteucci, G., Butters, D., Zhang, J., Castagna, J., 2005. Successful application of spectral decomposition technology toward drilling of a key offshore development well: 75th SEG meeting, Houston, Expanded Abstracts, 4: 262–264.
Falcon, N**.** L**.**, 1974. Southern Iran: Zagros mountains. In Spencer, A., Ed., Mesozoic–Cenozoic Orogenic Belts, Geological Society, London, Special Publications, https://doi.org/10.1144/ GSL.SP.2005.004.01.11., 4: 199–211.
Ford, D., Williams, P., 2007. Karst Hydrogeology and Geomorphology , John wiley & Sons, Ltd., The Atrium, Southern Gate, Chichester, West Sussex PO19 8SQ, England , 578: 1–578
Farsimadan, M., 2015. Image log Analysis of Well No. 52, Asmari Formation, Kupal oil Field, NISOC pub., P–8251, 65: 51–52 (in Persian)
Ghorbani, F., 2014. Fire extinguishing of Oil and Gas Wells, National Iranian South Oil Co. Pub., 245: 106–210 (in Persian)
Hosseini, A., Ziaii, M., Kamkar Rouhani, A., Roshandel, A., Gholami, R., J. Hanachi, J., 2011. Artificial intelligence for prediction of porosity from seismic attributes: Case study in the Persian Gulf, Iranian Journal of Earth Sciences 3, 7: 168–174.
Jahnert, R., Collins, L., 2012. Characteristics, distribution and morphogenesis of subtidal microbial systems in Shark Bay, Australia, Marine Geology, 303–306, 115–136.
Jamaludin, S. N. F., Mubin, M., Abdul Latiff, A. H., 2017. Imaging of karst on buried Miocene Carbonate Platform, Jur. Earth and Environmental Science 88, 012011, doi:10.1088/1755–1315/88/1/012011, 8: 1–8.
James, G.A., Wynd, J.G., 1965. Stratigraphic nomenclature of Iranian Oil Consortium Agreement area. American Association of Petroleum Geologists Bulletin, 49: 2182–2245.
Koson, S., Chenrai, P., Choowong, M., 2014. Seismic Attributes and Their Applications in Seismic Geomorphology, Bulletin of Earth Sciences of Thailand 6 (1, 9): 1–9.
Liu, J., Marfurt, K. J., 2007. Instantaneous spectral attributes to detect channels, Society of Exploration Geophysicists, vol. 72, 9: 23–31.
Mallat, S., Zhang, Z., 1993. Matching Pursuit with Time–Frequency Dictionaries. IEEE Trans Sig. Proc., 41: 3397–3415.
McClay K.R., Shaw J., Supp, J., 2011. Introduction to Thrust Fault Related Folding, AAPG., Memoir 94, 20: 1–20.
McQuillan, H., 1991. The role of basement tectonics in the control of sedimentary facies, structural pattern and salt plug emplacements in the Zagros Fold Belt of southwest Iran, Journal of Southeast Asian Earth Sciences, 5: 453–463.
Mehrabi, H., Rahimpour–Bonab, H., Al–Aasm, I., Hajikazemi, E., Esrafili–Dizaji, B., Dalvand, M., Omidvar, M., 2018. Paleo–exposure surfaces in the Aptian Dariyan Formation, offshore SW Iran: geochemistry and reservoir implications. Journal of Petroleum Geology, 41: 467–494.
Motiee, H., 1995. The Zagros Oil Geology, Vol. 1 & 2, The Geology Department of Iran, 1024: 1–1024. (In Persian)
Nasiri, M., Ehsani, F., 2014. The Rock properties Analysis of Asmari Reservoir, Kupal oil field, National Iranian South oil co., Report No. P–7996, 143: 1–143. (in Persian)
Nawab, S., Quatieri, T., 1988. Short–time Fourier transform. In: Lim, J. & Oppenheim, A. (Eds.) Advanced topics in signal processing. Prentice Hall Signal Processing Series, 289–337.
Omidpour, A., Amini, A., Jafari, J., 2006. Facies Analysis & Sedimentary Environment of Asmari Fm. in Kupal oil field, Geological Survey of Iran., 9: 1–9. (in Persian)
Oyeyem, K.D, Aizebeokhai, A.P., 2015. Seismic attributes analysis for reservoir characterization; Offshore Niger Delta, Petroleum & Coal 57(6), 10: 619–628.
Parham, S., Kamali, M.R., Fayazi, F., 2010. Petrography, Geochemistry and Reservoir Characterization of Dolomicrites in the Upper Member of the Dalan Formation, Persian Gulf, Iran, The 1st International Applied Geological Congress,

Department of Geology, Islamic Azad University of Mashhad, Iran., 6: 1–6.

Qi, J., Zhang, B., Zhou, H., Marfurt, K., 2014. Attribute expression of fault–controlled karst – Fort Worth Basin, Texas: A tutorial, Society of Exploration Geophysicists and American Association of Petroleum Geologists, 20: 1–20.

Raef, A.E., Mattern, F., Philip, C., Totten, M.W., 2015. 3D seismic attributes and well–log facies analysis for prospect identification and evaluation: Interpreted palaeoshoreline implications, Weir man Field, Kansas, USA, Journal of Petroleum Science and Engineering, 12: 1–12.

Rahimpour–Bonab, H., Eskandar, A., Sonei, R., 2009. Effects of the Permian–Triassic boundary on reservoir characteristics of the South Pars gas field, Persian Gulf. Geological Journal, 44: 341–364**.**

Rahimpour–Bonab, H., Mehrabi, H., Enayati–Bidgoli, AH., Omidvar, M., 2012. Coupled imprints of tropical climate and recurring emergence on reservoir evolution of a mid–Cretaceous carbonate ramp, Zagros Basin, southwest Iran. Cretaceous Research 37: 15–34.

Rahimpour–Bonab, H., Mehrabi, H., Navidtalab, A., Omidvar, M., Enayati–Bidgoli, AH., Sonei, R., Sajjadi, F., Amiri–Bakhtiar, H., Arzani, N., Izadi–Mazidi, E., 2013. Paleo–exposure surfaces in Cenomanian–Santonian carbonate reservoirs in the Dezful embayment, SW Iran. Journal of Petroleum Geology 36 (4): 335–362.

Ramsay, J. G., Huber, M. I., 1987. The techniques of modern structural geology, Vol.2, Folds and Fractures, Pergamon Press, London., 374: 1–374

Roghanian, R., Farazmand, M., 2008. Updating simulator model of Asmari reservoir: Kupal oil Field, National Iranian South Oil Company, Report No. P–6313, 145: 1–145. (in Persian)

Sepehr, M., Cosgrove, J.W., 2004. Structural framework of the Zagros Fold–Thrust Belt, Iran, Marine and Petroleum Geology, 21 (15): 829–843.

Sepehr, M., Cosgrove, J.W., Coward, M.P., 2002. The major fault zones Zagros controlling the sedimentation, deformation and entrapment of Hydrocarbon in the fold thrust belt, Iran, AAPG Annual Meeting March 10–13, Huston, Texas., 4: 1–4.

Shamsuddin, A., Ghosh, D., Shahar S., 2017. Geological features based on Spectral Decomposition: Techniques and examples from the Malay Basin, IOP Conf. Series: Earth and Environmental Science, 88 (2017) 012002 doi:10.1088/1755–1315/88/1/012002, 7: 1–7.

Sherkati, S., Letouzay, J., 2004. Variation of structural style and basin evolution in the central Zagros (Izeh zone and Dezful Embayment), Iran: Marine and Petroleum Geology, 21: 535–554.

Sherkati, S., 2005. Tectonics of sedimentary cover and basement in the Zagros Orogenic belt, Notes on Geometric Modeling of Deformation. NIOC Geological Report NO. 2067 (unpublished), 66: 1–66

Shinn, E.A., 1983. Bird's eyes, fenestrate, shrinkage pores, and loferites: A reevaluation, Sediment Petrology, 53: 619–628.

Skirius, C., Nissen, S., Hakell, N., Marfurt, K., Hadley, S., Ternes, D., Michel, K., Regler, I., D'Amico, D., Deliencourt, F., Romero, T., D'Angelo, R., Brown, B., 1999. 3D seismic attributes applied to carbonates, Jur. Of The Leading Edge, 8: 1–8.

Speers, R.G., 1976. Review of the geology of the Asmari reservoir–Kupal Field, Report No. P–3107, Exploitation Geology Division, Oil Service Company of Iran, Ahvaz, 28: 1–28.

Stöcklin, J., 1968. Structural history and tectonics of Iran: A review, American Association of Petroleum Geologists Bulletin, 52: 1229–1258.

Tucker, M.E, 1991. Sequence stratigraphy of carbonate–evaporate basins: models and application to the Upper Permian (Zechstein) of northeast England and adjoining North Sea, Journal of the Geological Society, London, 148: 1019–1036.

Zhu, H., Zhu X., Chen, H., 2017. Seismic characterization of Hypogenic karst systems associated with deep hydrothermal fluids in the Middle–Lower Ordovician Yingshan formation of the Shunnan Area, Tarim Basin, NW China , Hindawi Geofluids, Article Id: 8094125, 13: 1–13.

Ziegler, M.A., 2001. Late Permian to Holocene paleofacies evolution of the Arabian Plate and its hydrocarbon occurrences, GeoArabia (Manama), 6 (3): 445–504